

AN INTEGRATED FRAMEWORK FOR RISK AND IMPACT ASSESSMENT OF SEDIMENT HAZARD DISRUPTION ON A ROAD NETWORK

Johan Rose SANTOS¹, Varghese VARUN², Makoto CHIKARAISHI³, and Tatsuhiko UCHIDA⁴

¹Associate member of JSCE, Engineer II, Department of Public Works and Highways (DPWH - Bureau of Maintenance 201 2nd Street, Port Area, Manila, 1018, Philippines)
E-mail: jrasantos22@gmail.com

² Associate member of JSCE, Researcher, Graduate School of Advanced Science and Engineering, Hiroshima University
(1-5-1 Kagamiyama, Higashi-Hiroshima City, Hiroshima, 739-8529, Japan)
E-mail: varunv@hiroshima-u.ac.jp

³Member of JSCE, Associate Professor, Graduate School of Advanced Science and Engineering, Hiroshima University
(1-5-1 Kagamiyama, Higashi-Hiroshima City, Hiroshima, 739-8529, Japan)
E-mail: chikaraishim@hiroshima-u.ac.jp (Corresponding Author)

⁴Member of JSCE, Associate Professor, Graduate School of Advanced Science and Engineering, Hiroshima University
(1-5-1 Kagamiyama, Higashi-Hiroshima City, Hiroshima, 739-8529, Japan)
E-mail: utida@hiroshima-u.ac.jp

Road transport is one of society's most important lifeline especially during calamities and disasters. Conversely, natural disasters disrupts the road network which severely affects its functionality. In order to maintain the road network's functionality, it is crucial to determine the underlying risks that threaten it. Risks may exist from the (1) topological structure of road networks and (2) potentially from the natural hazard which roads are exposed to. Few road network vulnerability studies that incorporated risk assessment have evaluated the threats, impact and risk of natural hazards to the road network. This study proposes an integrated framework to assess risk of sediment hazard to the road network by borrowing concepts from (1) transport vulnerability studies; (2) risk assessment; and (3) spatial risk analysis, and applied it to an identified vulnerable road network in Kure City, Japan. The proposed risk framework involves the processes of topological network vulnerability analysis, exposure spatial analysis, hazard occurrence probability estimation through binary logit regression, impact calculation using Monte Carlo simulation and risk estimation. In this study, 12,000 possible multi-link disruption scenarios were simulated using the recorded sediment disaster information and rainfall event on July 2018 in Hiroshima prefecture. High probable to hazard and high impact links, i.e. critical links, in the road network were identified using the occurrence probability map, impact map and risk map generated from the framework. The policy implications of the generated maps may support in road mitigation and recovery prioritization during disaster, road infrastructure investment through risk-benefit analysis, and improvement of road transport's internal and external connectivity.

Key Words : *Road topological vulnerability, Road network disruption, Risk assessment, July 2018 Hiroshima sediment disaster, Monte Carlo simulation*

1. INTRODUCTION

Road transportation serves a vital function in the society. It does not only provide mobility services for passengers and goods, but also serves as the most important lifeline whenever a disaster occurs^{1) 2) 3)}. Roads facilitate disaster response and recovery activ-

ities including evacuation, rescue, and relief distribution²⁾. Likewise, it also assists in the repair and restoration of other important infrastructure systems such as telecommunication, power, and water supply⁴⁾.

However, roads also become the primary victim whenever a calamity happens. Disruptions caused by natural disasters hamper the road network's capability to perform its most basic function⁵⁾. With the

worsening condition of climatic events these recent decades manifested by frequent torrential rains and unpredictable weather patterns, natural hazards pose a greater threat making the road network more vulnerable.

It should be recognized that determining road transport vulnerability in the infrastructure sector management is vital as it also contributes to the improvement of a society's economy and over-all welfare¹⁾. Given the importance that the road network contributes to the society, it becomes a critical infrastructure that should be protected. Then, in order to maintain the functionality of road networks, it is crucial to determine the underlying risks that threaten it. Risks may exist internally and externally to the road network. Risks that are internal originate from the topological vulnerability within the road network structure. Meanwhile, the external risks may be caused by disruptions from accidental events (traffic accidents, natural disasters) or intentional acts (road repairs, strikes, terrorism)²⁾.

In this study, risks are quantified from existing risks on the road network's topological structure and the potential risks from natural hazard disruption. This study will contribute to the transport vulnerability studies that incorporated the concept of disaster risk assessment. Studies in the past have evaluated the threats, impacts and risk of natural hazards to the road network^{3,6-9)}.

However, these studies have several limitations regarding the risk assessment scope. The first limitation is that the case road network investigated in previous studies was either only focused on a portion of the network, or a simplified network^{3,6,8,9)}, and as a result it was not possible to reflect the entirety of the road network. This is due to complexity and computational requirement to make a complete risk assessment of the whole road network. Consequently, since only a portion of the road network was evaluated, the vulnerability of the road network from its topological structure was not completely evaluated. Second, the occurrence probability of a natural hazard or disruption was not emphasized, while the number of potential disaster scenarios was limited to one or two events^{6,8,9)}. Lastly, the impact calculation was obtained from a single link failure that may not truly reflect the actual scenario when a real disaster event occurs^{8,9)}.

To address the identified research gaps among the literatures reviewed, this study aims to propose a general framework to assess the risks from the topological structure of road networks and from natural hazards which roads are exposed to. The proposed framework borrowed concepts from three (3) different fields, namely, (1) transport vulnerability studies; (2) risk assessment; and (3) spatial risk analysis. The

proposed framework also provides a more holistic evaluation of risk that incorporates the topological network vulnerability, road network hazard exposure, hazard occurrence probability, and multi-link disruption impact on road network. To test the applicability of this framework, the study focuses on one type of hazard particularly sediment hazard, and conducted a case study using an identified vulnerable road network, Kure City, among 69 cities in Japan assessed by Santos et al. in their study¹⁰⁾. Kure City is also characterized with mountainous and island regions located in Hiroshima prefecture.

Meanwhile, for the estimation of hazard occurrence probability and simulation of multi-link disruption scenario, the study investigated a past sediment disaster event caused by torrential rains on July 2018 in Hiroshima prefecture. This disaster event severely disrupted the road network and isolated Kure City from outside connection and hampered disaster relief operations¹¹⁾. Therefore, the final output of the framework was a risk map that identified the critical road segments in Kure City, based on topology and hazard exposure.

The risk map's contribution is threefold: First, it can be used for disaster mitigation and recovery in the road network. Critical links that are exposed to natural hazards and greatly impact the functionality of roads may be strengthened and recovered before, after or during a disaster. Second, it can help facilitate road infrastructure investment. With the local government's limited resources, the risk map may aid in the proper allocation of road investment in road planning, construction or expansion. Cost-benefit analysis which is the primary basis of infrastructure investment may be shifted or complemented with risk-benefit analysis as well. Lastly, it may also support the improvement of road transport connectivity by determining how efficient or vulnerable a road network with its existing condition.

The remainder of this study is divided into four chapters. The second chapter reviews literature related to the concept of road transport vulnerability, disaster risk management and risk assessment, and how these fields have contributed to the conceptualization of the proposed risk framework for road networks. The third chapter discusses in detail the data used, study area and the application of the proposed risk framework. The results, discussion and generated maps are explained in the fourth chapter. Finally, the last part includes the summary, conclusion and policy implications of this study.

2. LITERATURE REVIEW

This literature review discusses three main concepts related to the formulation of the proposed risk framework. The first section discusses the topic of ‘vulnerability’ in road network studies, the second part explains the concept of ‘risk’ in disaster management, and the third part focuses on several road network vulnerability studies incorporating risk assessment.

(1) Vulnerability of road networks

Vulnerability has no generalized definition and its meaning mainly depends on the field of research²⁾. In the field of transport studies, a definition of vulnerability as the “susceptibility to incidents that can result in considerable reductions in road network serviceability” was provided by Berdica¹⁾. Almost two decades later, this definition has become the basis of numerous vulnerability studies focusing on the road network.

Mattson and Jenelius (2015) classified these vulnerability studies into two approaches: (a) *topological vulnerability*; and (b) *system-based vulnerability*. Topological vulnerability studies were founded from graph theory wherein the road transport system is represented as a network with road segments as ‘links’ and intersections as ‘nodes’^{2,5)}. On the other hand, system-based vulnerability focuses on the relationship between the demand and supply side of the road network²⁾. Both approaches follow a three-step network analysis which includes (1) defining a transport network; (2) formulating a disruption event; and (3) assessing the impact of the event disruption through an established or proposed index^{1,9)}. This study will emphasize vulnerability from the the topological approach.

a) Topological based method

This vulnerability analysis approach considers the network topology of a transport system and its characteristics, wherein network topology pertains to the physical structure and connectedness of the links and nodes in a road network⁵⁾. The motivation behind the study of road network topology stems from the maxim that “the structure affects function”⁵⁾. Consequently, any degradation or improvement in the road network structure, or any loss or failure in its components (i.e. links and nodes), will have a significant impact on the operation, serviceability, and functionality of the system^{4,5)}.

In order to measure the vulnerability of networks, several indices are used by different topological studies such as network efficiency¹²⁻¹⁴⁾, centrality measures (degree centrality and betweenness centrality)^{5,13,15)}, average path length^{6,14)}, clustering coefficient^{14,15)}, duality graphs¹³⁾, network robustness in-

dex¹⁶⁾, network trip robustness¹⁷⁾, annual travel delay¹⁸⁾ and average travel load and user travel time⁶⁾.

As topological vulnerability of road network is mainly concerned with the identification of critical components in the network (i.e., links or nodes) that will yield the highest impact when disrupted, main aspects that are studied are (1) network efficiency and (2) centrality measures^{4,6)}. In this study, the global network efficiency index as formulated by Latora and Marchiori (2001) will be utilized to measure the impact of disruption of a link thereby emphasizing its role in maintaining connectivity in the network. This will be discussed in detail on the methodology part.

b) Disruptions

An ‘incident’, which is used synonymously to *disruption* in this study, is defined as a failure or occurrence that causes significant functionality or serviceability degradation in a road network and its components^{1,4)}. The causes of disruptions on transport systems can be categorized either as internal or external, and as accidental or intentional²⁾. In the context of road network system, common incidents or disruptions can be summarized according to the proposed characterization of Mattson and Jenelius²⁾ (see Table 1). Among these disruptions, adverse weather conditions and natural disasters, along with traffic accidents, are identified as the most common in the road network⁴⁾.

Table 1 Characterization of incidents or disruption on a road network system

| Causes | Accidental events | Intentional interferences |
|----------|---|--------------------------------------|
| Internal | Traffic accident, bridge and pavement failure | Road repairs, traffic signal control |
| External | Adverse weather, natural disasters | Strikes, sabotage, terrorism |

c) Natural disaster disruptions

This type of disruption is classified as an external-accidental incident caused by adverse weather or natural disasters, including torrential rains, storms, flood, snowfall, landslides, volcanic eruptions, and earthquakes²⁾. These natural disaster disruptions can be investigated through either a single link or node failure^{9,19)}, or area-based disruption²⁰⁾.

The study of Dalziell and Nicholson³⁾ is one of the earliest vulnerability studies to examine the impacts of accidental disruptions on the road network. They investigated multiple hazard threats such as snow and ice, volcanic eruption, earthquakes and traffic accidents, and the resulting impact of road closure on Desert Road, New Zealand. Following this seminal study, several transport vulnerability studies have

emerged incorporating natural disasters, either focusing on individual types of hazards including floods, earthquake¹⁹⁾, landslides (sediment hazard)^{9,21)}, or multi-hazard combination^{7,8)}. Accordingly, this study focuses on sediment hazard as a potential disruption on the road network.

d) Sediment hazard disruption

Sediment hazard, commonly known and generalized as landslides, is defined as “the movement of a mass of rocks, debris or earth down a slope”²²⁾. Factors that determine the occurrence probability of sediment hazard includes (1) *preparatory variables* which include the area’s geology, slope, elevation and vegetation cover; and (2) *triggering variables* such as heavy rainfall, earthquakes, deforestation and slope excavation²²⁾. However, transport network vulnerability studies that have focused on the impact of sediment disaster as a potential disruption to the road network did not consider these triggering variables in their evaluations^{7-9,21)}. In this study, it is argued that sediment hazard is not a disruption that occurs by itself. Triggering factors, such as heavy rainfall, should be examined as well to determine the risk of sediment disaster on the road network. This can be done by investigating past extreme rainfall events and pattern in that area.

Moreover, in the field of geology engineering, various methods to assess the occurrence probability of sediment hazard are classified into four approaches namely (a) inventory, (b) heuristic, (c) statistical, and (d) deterministic²²⁾. This study will utilize a combination of inventory and statistical methods. In inventory method, recorded past disaster location and geographical characteristics are compiled, investigated, and becomes the basis of hazard maps²²⁾. However, inventory method cannot identify potential locations unless the sediment hazard have occurred already²²⁾.

For this study, the limitation of inventory method will be supplemented by statistical approach. In the statistical approach, estimations are done for locations where sediment hazard has not yet occurred but has similar prevailing conditions with recorded sediment disaster sites²²⁾. In this case, an analysis that combines both the preparatory factor and triggering factor of sediment hazard will provide an insight on how to estimate occurrence probability and ultimately, the risk as well.

(2) Disaster risk assessment

In transport vulnerability studies, ‘risk’ is defined as the product of incident probability and the resulting impact from that incident^{1,23)}. Mattson and Jenelius (2015) extended this description and emphasized the incidence scenario. They claimed that risk refers to a triad that consists of the incident scenario,

incident probability and incident impact (see Fig.1)²⁾.



Fig.1 Risk triad in transport vulnerability studies. Adapted from Mattson and Jenelius²⁾



Fig.2 Interrelationship of disaster risk, hazard, exposure and vulnerability. Adapted from UNISDR²⁴⁾ and IPCC²⁵⁾

On the other hand, ‘risk’ in disaster management comprises a broader scope. The United Nations International Strategy for Disaster Reduction (UNISDR) (2009) defined risk as the possible harm, fatality, or asset damage from a probabilistic event expressed as the intersection of hazard, exposure and vulnerability²⁴⁾. The interrelationship of risk to the concepts of hazard, exposure and vulnerability is illustrated in Fig.2.

In order to connect the concept of ‘risk’ from the fields of transport vulnerability studies with disaster risk assessment, consideration should be given to the concept of ‘hazard’ (see Fig.2). In real world scenarios, hazards caused by weather and climate events can be considered similar to the natural ‘incidents’ (see Fig.1) that occur in the road network. Hence, this vulnerability study aims to propose a more comprehensive framework assessing the risk of a defined incident and hazard (sediment disaster) on a road network by incorporating the concept of risk assessment.

(3) Road network vulnerability studies incorporating risk assessment

This study is not the first to combine the concept of disaster risk assessment into transport vulnerability studies. Dalziell and Nicholson (2001), Jenelius et al. (2006), Tacnet et al. (2012), Michal et al. (2014), and Postance et al. (2017) are among the few road network vulnerability studies that incorporated risk assessment in their own novel studies^{3,6-9)}.

Dalziell and Nicholson's³⁾ risk assessment of Desert Road locality in New Zealand involved the estimation of disaster probability using Monte Carlo simulation and impact calculation using closure cost. Meanwhile, Jenelius et al. (2006) focused on the topological structure of the network in northern Sweden and calculated the impact of road closures in terms of increase in travel cost⁶⁾. Tacnet et al.⁷⁾ proposed a risk assessment methodology heavily focused on the topological structural analysis of the Maurienne Valley road network in France. A risk assessment of natural hazards for the road network was also provided by Michal et al.⁸⁾ who studied the road vulnerability and combined threat of multi-hazard. Lastly, Postance et al.⁹⁾ conducted an impact assessment of landslide disruption on the national roads of Scotland.

However, these studies have several limitations regarding the risk assessment scope. The first limitation is that the case road network investigated in these studies was either only focused on a portion of the network, or a simplified network^{3,6-9)}. Dalziell and Nicholson³⁾ only evaluated the closure of few main highways in Desert Road. Jenelius et al.⁶⁾ used a simplified Swedish road network by dividing it into municipality zones. Michal et al.⁸⁾ also simplified the road network in Luhacovice in Czech Republic in their study. Similarly, Postance et al.⁹⁾ only included main arterial roads in Scotland in their analysis. The reason behind this trend among the reviewed studies might be due to the complexity and computational requirement to make a complete risk assessment of the whole road network. Consequently, since only a portion of the road network was evaluated, the vulnerability of the road network from its topological structure was not completely evaluated. Second, the occurrence probability of a natural hazard or disruption was not emphasized, since the number of potential disaster scenarios was limited to one or two events. Jenelius et al.⁶⁾ only assumed the average and worst-case scenario with regards to road closure in their study. Lastly, the impact calculation was obtained from a single link failure as employed by Michal et al.⁸⁾ and Postance et al.⁹⁾ (2017) in their studies. However, single link failures may not truly reflect the actual scenario when a real disaster event occurs.

On the other hand, Taylor⁴⁾ indicated a gap in top-

ological analysis as it may not reflect the road network's physical characteristics and potential exposure to natural hazards. Hence, this research recommends a more holistic and integrated approach to risk assessment by proposing a framework that incorporates the topological network vulnerability, road network hazard exposure, hazard occurrence probability, and multi-link disruption impact on road network for sediment hazard to define the risk as presented in Fig.3. This framework was adapted from Ferretti and Montibeller's²⁶⁾ components of spatial risk maps, which was used to assess the environmental multi-impacts in a flood-prone location in northern Italy. Their risk framework was based on the multi-attribute utility theory where the impact of flooding was measured through the social, economic and environmental disutility. They assessed the over-all risk as the product of the spatial probability, spatial vulnerability and impact.

Meanwhile in this study, Ferretti and Montibeller's²⁶⁾ spatial risk framework is tailored fit specifically to road networks. It was modified to accommodate the vulnerability of road networks measured from their topological characteristics borrowing the concept from transport vulnerability studies. In addition, the exposure layer was added to take into consideration the existing threat of sediment hazard in the road network from the disaster risk management perspective. The detailed discussion of each step in the framework is provided in the next section.

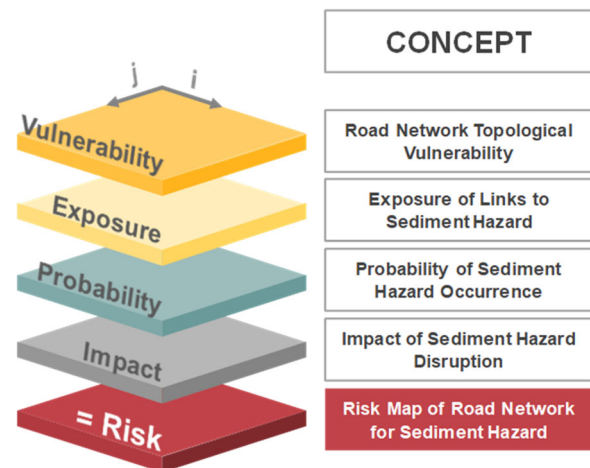


Fig.3 Road network risk assessment framework for sediment hazard. Modified from Ferretti and Montibeller²⁶⁾

3. METHODOLOGY

This chapter is divided into three parts. The first part lists all the dataset and tools used, while the second part presents the study area and the reason for its selection. The last part discusses the proposed risk

framework, and the processes employed for the research methodology.

(1) Dataset and tools

The list of the dataset and sources used in this study is enumerated in Table 2. In order to apply the proposed risk framework, individual layers from four (4) datasets extracted from different sources were generated for the spatial analysis.

The first essential dataset layer is the GIS information of the road network and its components. The second layer is the sediment hazard maps utilized in the exposure process. The third and final layers are recorded data from the sediment disaster on July 2018 including the sediment disaster locations and rainfall amount distribution used for the occurrence probability calculation. All the layers generated were processed through ArcGIS. Other mapping processes and spatial analysis were done through ArcGIS as well. Meanwhile, statistical computations were conducted through Rstudio program. The next section focuses on the study area, Kure City.

Table 2 Dataset description and sources

| Data | Description | Source |
|---|--|--|
| 1. Kure City Road Network Data | GIS information of road network including nodes, links, road length, road type and coordinates | Japan ESRI Road Network Data Collection 2015 |
| 2. Sediment Hazard Maps | GIS hazard maps of potential location of debris flow, debris flow hazard area and watershed boundary (catch basin) | Hiroshima Prefectural Government - Earth and Sediment Disaster Caution Area ²⁷⁾ |
| 3. July 2018 Disaster Information | GIS map of debris starting point and debris flow locations on July 2018 sediment disaster in Hiroshima Prefecture | Geospatial Information Authority of Japan ²⁸⁾ |
| 4. Rainfall Amount on July 2018 Disaster | Maximum R' values on a 10-minute interval from July 6, 18:00-21:00, to July 7, 3:00-6:00, 2018 sediment disaster in Hiroshima Prefecture, Chugoku Region | DIAS-XRAIN data ²⁹⁾ |

(2) Study area

The case study selected for this research is an identified vulnerable road network, Kure City, situated in Hiroshima Prefecture, Japan. Kure City road network consists of 18,125 links and 14,276 nodes with a total

road length of 1,679.087 km and area of 356.41 sq.km. (see Fig.4). All road types ranging from city roads to national expressways were included in the topological network analysis.

Moreover, according to the study of Santos et al. (2020), Kure City ranked as the least efficient road network and 2nd to the least robust city against random attack among all the 69 Japanese cities studied¹⁰⁾. A comparative illustration of the global efficiency of the 69 Japanese cities is shown in Fig.5.

Aside from having a vulnerable road network, Kure City is also a vulnerable city exposed to the danger of sediment hazard. It has frequently experienced sediment related disasters throughout the decades due to its location on the mountainous and coastal regions of Hiroshima prefecture. The latest sediment disaster event that happened on July 2018 due to torrential rains caused numerous injuries, fatality and damage to property. The disaster event also severely disrupted the road network that isolated the whole city from outside connection and hampered disaster relief operations¹¹⁾. For these reasons, the proposed risk framework was applied methodologically to Kure City as discussed on the following section.

(3) Research methodology

The research methodology employed for this study is the application of the proposed risk framework in Kure City. Fig.6 summarizes the different concepts and processes involved at each step of the framework, while the detailed discussion is provided in the subsequent sections.

a) Vulnerability

The first step of the framework is determining the topological characteristics and vulnerability of the road network. Topological vulnerability of road network is mainly concerned with the identification of critical components in the network (i.e., links or nodes) that will yield the highest impact when disrupted^{4,6)}. Topological vulnerability focuses on the importance of each network component and its role in maintaining connectivity. Main aspects that are studied in topological vulnerability are (1) network efficiency and (2) centrality measures⁴⁾.

In this study, the main vulnerability indicator used is the network efficiency that measures how a system facilitates movement, or indicates how the network is interconnected [4]. It is calculated as:

$$E(G) = \frac{1}{N(N-1)} \sum_{i \neq j \in G} \frac{1}{d_{ij}} \quad (1)$$

Where, $E(G)$ represents the average efficiency of a network, N represents the total number of nodes in

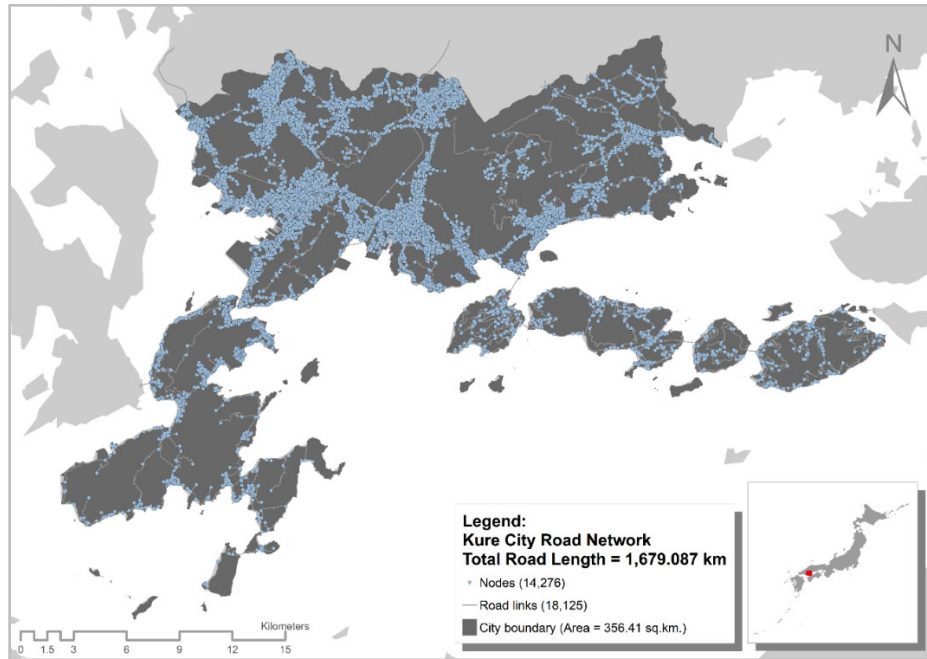


Fig.4 Kure City road network

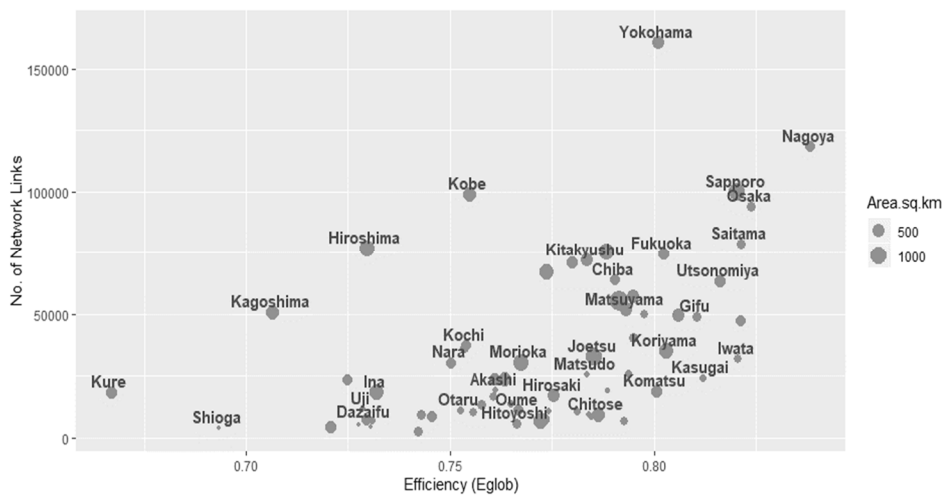


Fig.5 Global efficiency of 69 Japanese cities. Reprinted from “Road Network Vulnerability and City-level Characteristics: A Nationwide Comparative Analysis of Japanese Cities”¹⁰⁾

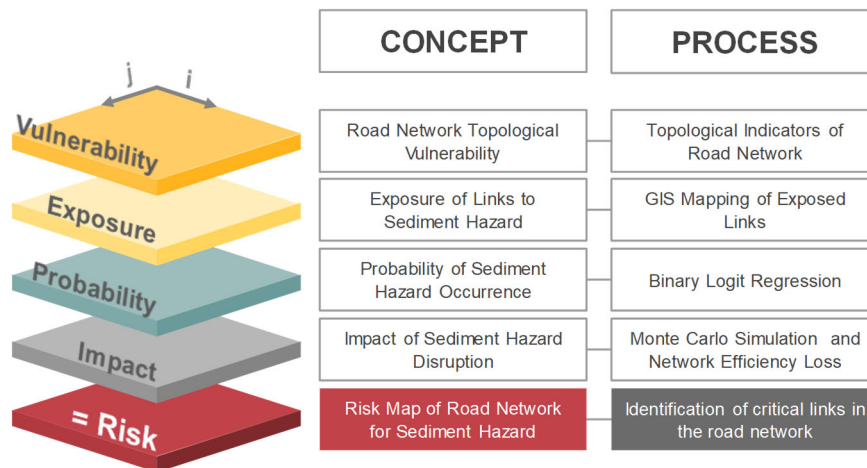


Fig.6 Proposed risk framework concepts and processes

the network, and d_{ij} represents the geodesic distances between any node pair $i - j$. In order to utilize this index to compare different sized networks, or the specified network itself in varied states, Latora and Marchiori (2001) proposed a normalization formula to calculate for the global network efficiency by dividing $E(G)$ by $E(G_{id})$ which represents the ideal graph using the Euclidean distances instead of the geodesic distances between any node pair $i - j$.

The global network efficiency is represented as^{4,12)}:

$$E_{glob} = \frac{E(G)}{E(G_{id})} \quad (2)$$

Topological measures were also calculated to indicate the topological characteristics of the road network which include (a) network complexity; (b) degree of connectivity; and (c) average degree. First, the network complexity ("β") signifies the inherent complexity of the network calculated as the ratio of the total number of links (L) to the total number of nodes (N) in the network, or simply³⁰⁾:

$$\beta = \frac{|E|}{|N|} \quad (3)$$

Second, the degree of connectivity ("γ") of planar networks which signifies the actual connectedness to potential connectedness in the road network, computed as³⁰⁾:

$$\gamma = \frac{|E|}{3(|N| - 2)} \quad \text{where: } |N| \geq 3 \quad (4)$$

Lastly, the average degree ("C^D") indicates the average number of direct connections from a node to all other nodes in the network¹²⁾ where k_i is the degree of node i , and calculated as:

$$C^D = \frac{1}{|N|} \sum_i k_i \quad (5)$$

After measuring the topological characteristics of the road network using its components, e.g. links and nodes, the next step is to determine the exposure of each road links to sediment hazard.

b) Exposure

In this step, the exposure of road links to sediment hazard was determined using hazard maps of potential debris flow locations and debris flow damage hazard area obtained from the Hiroshima Prefectural Government²⁷⁾. The watershed boundary area, or water run-off catch basins, of mountainous sections in Kure City was extracted as well. The potential debris flow locations, debris flow damage hazard area, and

watershed boundaries indicate the geographic characteristics and soil morphology of Kure City which may be considered as part of the preparatory factors that determines the occurrence of sediment hazard²²⁾. After which, the road links exposed to potential debris flow, damage hazard area and watershed boundary (or the runoff catch basins) in Kure City were investigated using the overlay analysis in ArcGIS.

Figs. 7 and 8 show the generated map consolidating all these preparatory factors of sediment hazard in Kure City road network. The next section will discuss how these preparatory factors along with the triggering factor, rainfall, were used to measure the probability of sediment disaster occurrence.

c) Probability

The probability of sediment disaster is determined through the preparatory factors, as tackled in the previous section, and the triggering factor, rainfall in this case. The rainfall factor was extracted from the rainfall distribution which is a processed maximum R' values on a 10-minute interval from July 6, 18:00-21:00, to July 7, 3:00-6:00, 2018 in Hiroshima Prefecture, Chugoku Region. Nakai et al.³¹⁾ proposed and tested this rainfall index R' and found that it is more accurate compared to older rainfall indices used in estimating the occurrence probability of sediment disaster. Similarly, Kobashi et al.²⁹⁾ (2019) used this index in their study to investigate the debris flow occurrence in Hiroshima prefecture on July 2018. The calculated R' maximum values as computed in their study for Kure City is shown in Fig.9.

In the field of geology engineering, various methods to assess the occurrence probability of sediment hazard are classified into four approaches namely (a) inventory, (b) heuristic, (c) statistical, and (d) deterministic²²⁾. In this study, the method considered was a combination of inventory and statistical approaches. Using the inventory method, recorded locations of the recent sediment disaster from July 2018 were utilized. Fig.10 shows the sediment disaster (landslide) starting point locations within the satellite readable range, and the identified affected road links which are both included and not included in the existing exposure map (see Fig.7).

Subsequently, the statistical approach was conducted through a binary logit regression to determine the probability of occurrence or non-occurrence of sediment disaster on a road link using the preparatory factors (potential debris flow locations, debris flow damage hazard area, and watershed boundaries), and triggering factor (rainfall amount) as the explanatory variables. The model was fitted using the recorded sediment disaster locations and rainfall amount on July 2018 for Kure City for only 16,775 links of the total road links. This is due to the limited satellite

readable range and data acquired on July 2018 wherein the total city area of Kure was not covered (see Fig.10). The binary logit model is indicated as:

$$v_l = \beta_0 + \beta_1 X_{l1} + \beta_2 X_{l2} + \beta_3 X_{l3} \quad (6)$$

Where, v_l is the latent variable determining the degree of disruption of road link l , X_{l1} indicates if the road link l is within exposure hazard area or not [1,0], X_{l2} signifies if the road link l is within watershed boundary or not [1,0], and X_{l3} is the rainfall amount on road link l on July 2018. Consecutively, the occurrence probability of sediment disaster on road link l , OP_l , can be calculated using the formula:

$$OP_l = \frac{\exp(v_l)}{1 + \exp(v_l)} \quad (7)$$

The model is estimated by using the maximum likelihood estimation method where the likelihood function LL is defined as follows:

$$LL = \prod_l OP_l^{Y_l} (1 - OP_l)^{1-Y_l} \quad (8)$$

Where Y_l is equal to one if the road link was disrupted by debris flow on July 2018 disaster and otherwise, equal to zero. Finally, the estimated OP_l for each of the 18,125 links was used for the Monte Carlo simulation and impact calculation. This process will be explained in the succeeding section.

d) Impact

The impact of link disruption was quantified by observing numerous possible combinations of link failure when a sediment disaster occurs. Then, the network efficiency loss was measured at each scenario. Similar to previous transport vulnerability studies^{3,19}, this research used Monte Carlo simulation to generate 12,000 possible scenarios of road link disruption due to sediment disaster in Kure City. The Monte Carlo simulation process is shown in Fig.11.

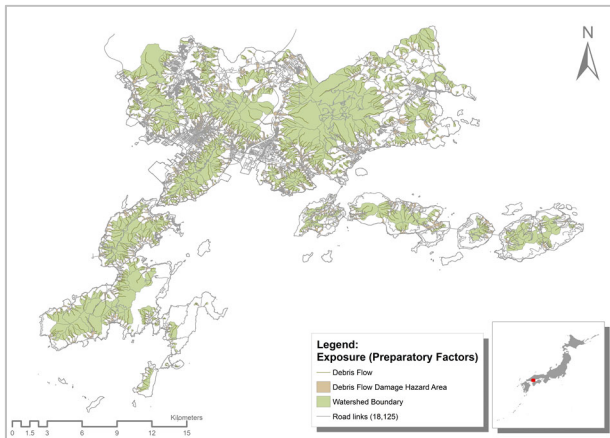


Fig.7 Kure City sediment hazard preparatory factors map

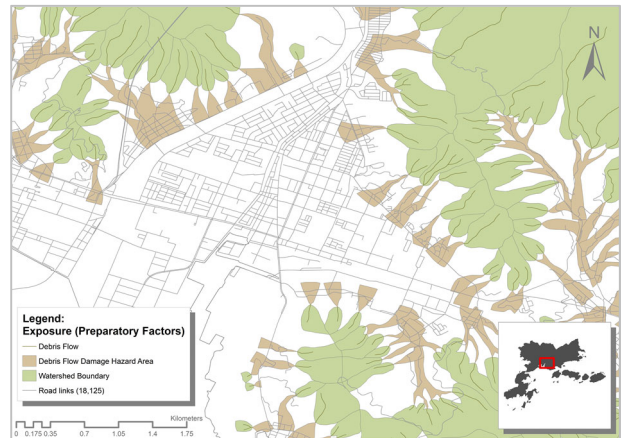


Fig.8 Kure City sediment hazard preparatory factors map (enlarged version)

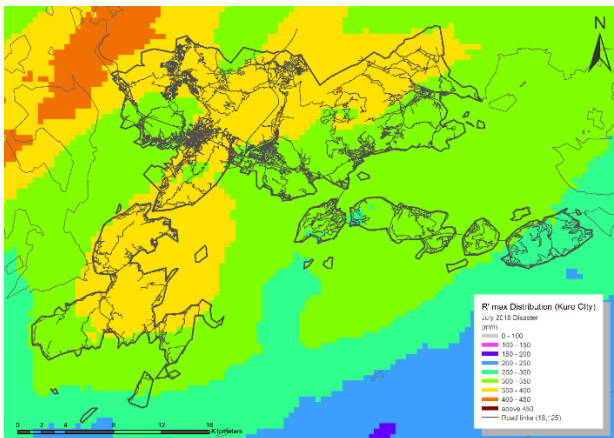


Fig.9 R' max distribution on July 2018 in Kure City. Source²⁹⁾

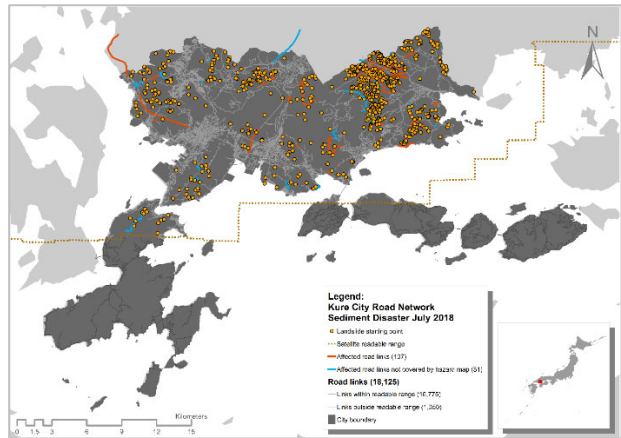


Fig.10 July 2018 sediment disaster location in Kure City. Source: Geospatial Information Authority of Japan²⁸⁾

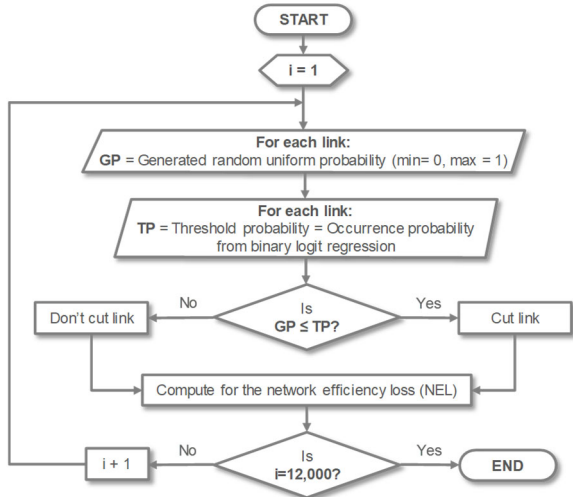


Fig.1 Monte Carlo simulation flowchart process

In order to compute for the network efficiency loss (NEL_i) at each iteration, the calculated efficiency at each iteration (E_i) is subtracted from the initial global network efficiency without any disruption (E_{glob}), or simply:

$$NEL_i = E_{glob} - E_i \quad (9)$$

Meanwhile, the impact of each road link to the network efficiency loss is computed as the average network efficiency loss per link ($AELL_l$), calculated as:

$$AELL_l = \frac{\sum [NEL_i]}{ND_{link\ l}} \quad (10)$$

Where, DL_i is the number of disrupted links per iteration, and $ND_{link\ l}$ is the total number of iterations where $link\ l$ was disrupted. After calculating the impact of each link in the network, the risk can be computed as discussed in the next passage.

e) Risk

The final process in the framework is the computation of risk. To calculate the average risk of sediment hazard per link in the road network, the occurrence probability (OP), from the binary logit regression, is multiplied to the average network efficiency loss per link (AELL), from the Monte Carlo simulation, or simply:

$$RISK_l = OP_l \times AELL_l \quad (11)$$

4. RESULTS AND DISCUSSION

This chapter contains the results and discussion including the risk map which is the final output of the

risk framework. The sections are sequenced from vulnerability, exposure, probability and impact, to the computation of the risk due to sediment hazard in Kure City’s road network.

(1) Vulnerability

The results generated from the network topological evaluation for Kure City are listed in Table 3. It shows that the calculated global network efficiency for Kure City is 0.690. While this value is higher compared to the results from a previous study by Santos et al. (2020) which is 0.667, Kure City remains the least efficient among various Japanese cities studied even after calibration (see Fig.5). A low network efficiency means that the interconnectedness of the network is low, or that the disconnectivity is high, leaving a vulnerable road network even without intervention or disruption.

Table 2 Results of network topological evaluation

| Topological Indicators | Value |
|--|--------|
| 1. Kure Road Network Topology | |
| Nodes | 14,276 |
| Links | 18,125 |
| Global network efficiency (E_{glob}) | 0.690 |
| 2. Network Indicators | |
| Network complexity (β) | 1.269 |
| Degree of connectivity (γ) | 0.423 |
| Average degree (C^D) | 2.539 |

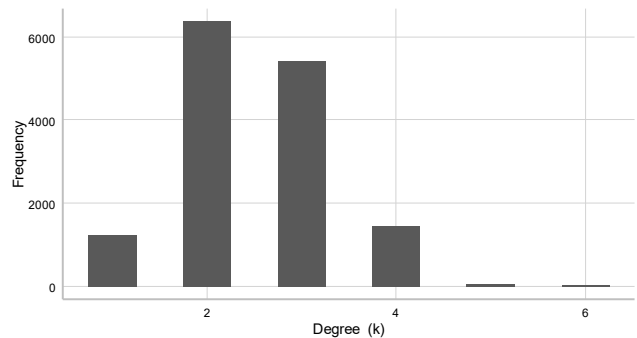


Fig.12 Degree distribution

Meanwhile, the average degree of connection at each node in the network is at 2.539, which suggests that in a single node there is at least 2 links connected to it. Fig.12 illustrates the degree distribution and frequency for each node degree (k). It can be observed that most nodes in the network have 2-3 links connected to it. Nodes with a degree of 1 may be considered as either cul-de-sacs, or boundary nodes that lie on the border of Kure City to adjacent cities or districts. Fig.12 also suggests that Kure City road network contains more than 1,000 intersections with a

degree node of 4. Also, several 5-6 links to node connection can be observed, and this suggests not only the importance of that high degree node but of the links connected to it as well.

Other road network indicators show that the network complexity of Kure City is moderately average at 1.269, and the degree of connectivity is at 42.3%. A connectivity degree of 42.3% suggests the actual connectedness in the road network has not yet even reached half of the potential connectedness. In comparison to other transport networks, these values fall under the first phase ($\beta \leq 1.30$, $\gamma \leq 0.50$) of a three-phase process that describes the network's 'state' as Derrible and Kennedy³⁰⁾ described it in their study wherein they evaluated 33 metro systems around the world.

Falling under a phase 1 category suggests that the network is still in the early stage of development and may still be expanded since it has not yet reached the maturity level (Phase 3) where the network complexity is approaching a value of 2.0 and the degree of connectivity is at least 66% connected³⁰⁾. However, these topological indicators would provide more insight if compared alongside with other city road networks like the efficiency indicator. Furthermore, unlike metro systems, the development and expansion of Kure's road network might be more difficult and hindered by geographic conditions because of its mountainous and island regions. The next section shows how this geographic landscape makes Kure City more vulnerable not only because of its road network, but also due to its exposure to sediment hazard.

(2) Exposure

Road links that were exposed to sediment hazard were identified using the existing hazard maps from the Hiroshima Prefectural Government and spatial analysis. Fig.13 shows that 5,585 of 18,125 road links, or about 31% of all the links were found to be exposed to sediment hazard. However, this maybe an underestimation as other road links may also be exposed similar to the event of the July 2018 disaster where 56 affected road links were not covered by the hazard maps (see Fig.10). This shows that inventory assessment may not be enough to establish a baseline to generate disaster probability scenarios, and all the road links in the network should also be evaluated. The next section explains the results of the occurrence probability computation using the exposure results and other explanatory variables in the binary logit regression.

(3) Probability

Before model fitting Equation (6), the correlation and multicollinearity of the explanatory variables, in-

cluding X_{I1} that indicates if road link l is within exposure hazard area or not, X_{I2} that signifies if road link l is within watershed boundary or not, and X_{I3} as the rainfall amount on road link l on July 2018, were measured first. The results are indicated in Table 4.

Table 3 Pearson correlation and multicollinearity among variables

| Vari- ables | Pearson correlation (r) | | | Multicollinearity Variance Inflation Factor (VIF) |
|----------------|-------------------------|----------|----------|---|
| | X_{I1} | X_{I2} | X_{I3} | |
| X_{I1} | | | | 1.003398 |
| X_{I2} | -0.014689 | | | 1.000237 |
| X_{I3} | 0.056251 | 0.003764 | | 1.003195 |

Table 4 Binary logit regression model comparison

| Model | Combination of Variables | Akaike Information Criterion (AIC) | Log- likelihood (LL) |
|-------|-----------------------------|---|----------------------------|
| 1 | $X_{I1} + X_{I2} + X_{I3}$ | 1192.644 | -592.321 |
| 2 | $X_{I1} + X_{I2}$ | 1195.517 | -594.7579 |
| 3 | $X_{I1} + X_{I3}$ | 1271.495 | -632.747 |
| 4 | $X_{I2} + X_{I3}$ | 1217.369 | -605.6836 |
| 5 | X_{I1} | 1274.158 | -635.0788 |
| 6 | X_{I2} | 1221.05 | -608.5248 |
| 7 | X_{I3} | 1293.07 | -644.5349 |
| 8 | intercept | 1297.047 | -647.5233 |

As per examination, it was found that there was negligible correlation ($r < 0.1$) and insignificant multicollinearity ($VIF < 5$) among explanatory variables. Afterwards, the best fit model was determined by measuring the lowest AIC among possible combinations of the explanatory variables as shown in Table 5. It was determined that model 1 showed the most accurate prediction, and the fitted binary logit regression model yielded the equation:

$$v_l = -9.189 + 1.025X_{I1} + 2.586X_{I2} + 0.009X_{I3} \quad (12a)$$

In this model, it was found that all the explanatory variables are significant to at least a confidence level of 95% (see Table 6). Moreover, all the variables demonstrate a positive relationship with the occurrence of debris flow (sediment disaster).

Consecutively, we computed the v_l , which is the degree of disruption in road link l and the occurrence probability of sediment disaster (OP_l) using equation (7) for all 18,125 links. Fig. 14 shows the occurrence probability distribution while Table 7 summarizes the calculated occurrence probability values among all links in the network. A map showing the occurrence probability of sediment hazard in Kure City road network is also provided in Fig. 15.

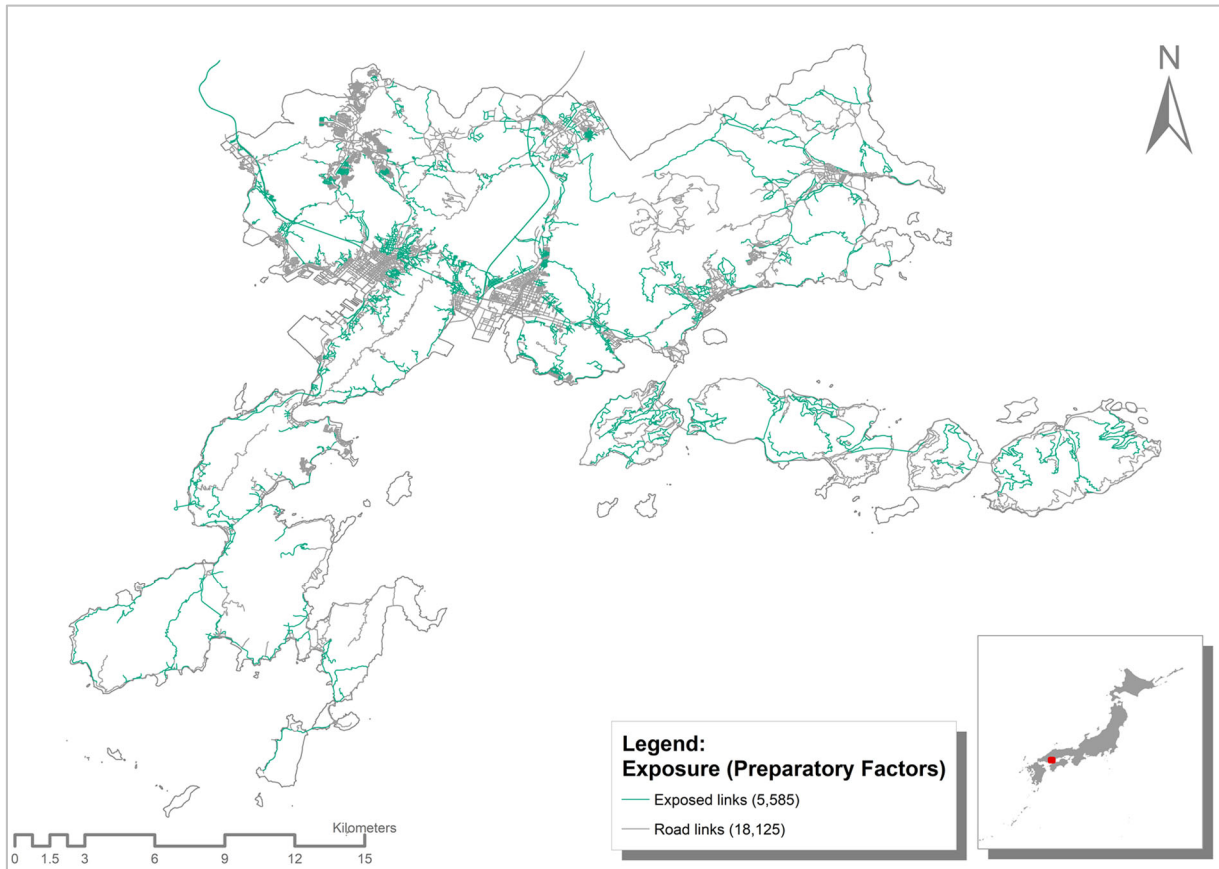


Fig.2 Sediment hazard exposure map to in Kure City map

Table 5 Binary logit model 1 estimation results (n=16,775)

| | Estimate | Z value | |
|-----------|----------|---------|-----|
| Intercept | -9.18928 | -5.705 | *** |
| X_{I1} | 1.025493 | 5.212 | *** |
| X_{I2} | 2.585618 | 11.237 | *** |
| X_{I3} | 0.009005 | 2.159 | * |

Significant codes: 0 ‘***’ 0.001 ‘**’ 0.01 ‘*’ 0.05 ‘.’ 0.1 ‘ ’

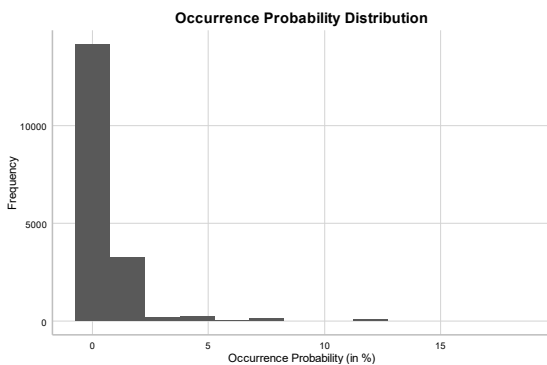


Fig.3 Distribution of Occurrence Probability of all links

Table 7 Occurrence probability (OP) values (n=18,125)

| Description | OP Value (in %) |
|-------------|-----------------|
| average | 0.6908608 |
| min | 0.1519572 |
| max | 17.8586 |

In Fig.15, the calculated occurrence probabilities were categorized into five by Jenks natural breaks classification in ArcGIS. Most of the links fall under the category 1 and 2 ($OP < 0.661311\%$) while links with category 4 and 5 ($OP > 1.979781\%$) are located near or on mountainous regions of Kure City.

Even though the occurrence probability map is consistent with the geographical characteristics of the region, it should be noted that this occurrence probability map is not an absolute reflection of the probability of sediment disaster in Kure City, but only provides one of the possible case scenarios when a similar rainfall amount of July 2018 disaster happens again. The next section discusses the impact calculation from Monte Carlo simulation results.

(4) Impact

The impact of each link, indicated as the average efficiency loss per link (AELL), was computed from the network efficiency loss (NEL) from 12,000 iterations using equation (10). To check the stability of the generated results, the simulation stability of 12,000 iterations was calculated using the error component of the computed AELL as shown in Table 8. The error component was computed by comparing the AELL calculated between group A and B with same number of iterations. While it is verified that the

results are quite stable at 12,000 iterations as suggested in Fig.16, the accuracy maybe furthered increased by increasing the number of iterations. How-

ever due to the computational requirement as each iteration requires around 42 seconds to complete, the number of simulations were limited to 12,000 simulations.

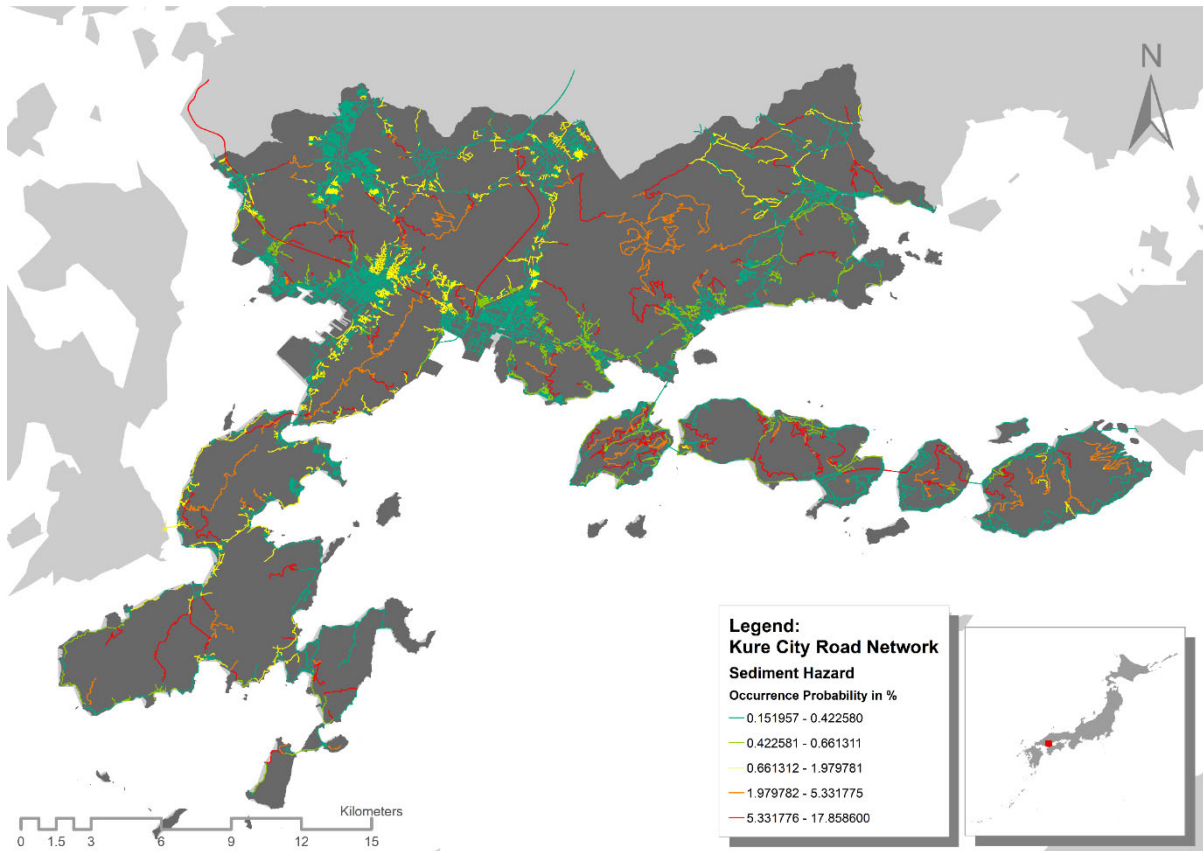


Fig.15 Occurrence probability of sediment hazard map in Kure City

Table 8 Simulation stability

| Iteration | $\sum (AELL_A - AELL_B)_i $ | $\sum (AELL_A - AELL_B)_i ^2$ |
|-----------|------------------------------|--------------------------------|
| 500 | 0.013532921 | 1.831400E-04 |
| 1000 | 0.009516265 | 9.055930E-05 |
| 3000 | 0.00561134 | 3.148714E-05 |
| 6000 | 0.003903819 | 1.523980E-05 |
| 12000 | 0.0028830376 | 8.311906E-06 |

Note: *AELL* – Average Efficiency Loss per Link

The results summary of the Monte Carlo simulation is provided in Table 9 where the NEL at each iteration and AELL are shown. Among the 12,000 simulations generated, iteration 3,560 was identified to have the highest impact with 17.13% NEL. Fig.18 shows the combination of 137 links disrupted in iteration 3,560. Meanwhile, the distribution of the average impact among all road links in Kure City is presented in Fig.19.

In Fig.19, it can be observed that most links fall under the middle impact category ($0.181858e-3 > AELL$

$>0.195512e-3$) with high impact links ($AELL > 0.213512e-3$) sparsely located around the city network. Segments of inter-city link connections including Route 31 (Hiroshima-Kure Road) and Route 375 (Higashihiroshima-Kure Expressway) were also identified as high impact links based on the network efficiency loss.

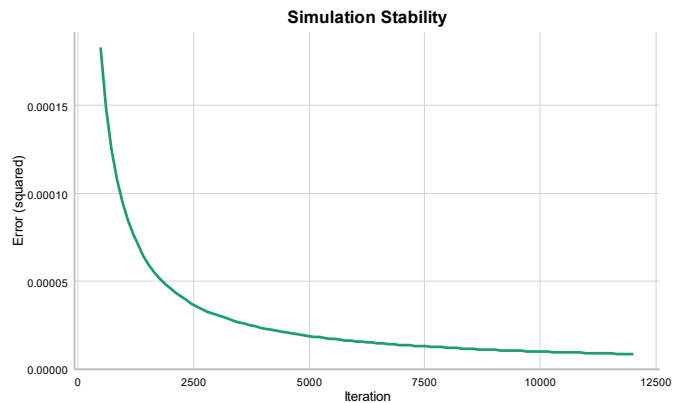


Fig.16 Number of iterations vs error in squared form

Meanwhile a comparative chart of the number of

disrupted links and the NEL in percentage for the 12,000 simulations, including the July 2018 disaster event, is shown in Fig.17. The NEL of the July 2018 disaster was estimated at 14.73%. While this is lower than the impact of iteration 3,560, the July 2018 disaster only disrupted 107 links (see Fig.10) compared to the 137 links in iteration 3,560. This provides an insight of the disaster’s severity and the importance of the links that were disrupted during that calamity. It also reveals that due to the unpredictability and nature of sediment disasters, simulations may be insufficient to cover the worst possible disaster scenario. In the last section, the risk of sediment hazard utilizing the results from the previous sections will be discussed.

(5) Risk

In this study, the risk of sediment hazard is defined as the product of disaster occurrence probability and the resulting impact when that disaster occurs. In the final step of the risk framework, the average risk for each link in the road network is computed using equation (11). Aside from the average risk, the minimum risk and maximum risk may also be calculated using the minimum and maximum impact for each link as shown in Table 10. Calculating the minimum and maximum risks along with the average risk may provide insights on the other possible outcomes when a specific link gets disrupted. Figs. 20, 21 and 22 show the distribution of the minimum, maximum and average risks among all links in Kure City road network.

Table 9 Monte Carlo sample simulation results

| Link | Occurrence Probability in % (OP_l) | Iteration (1= disrupted link, 0 = undisrupted link) | | | | | | | | | Average Efficiency Loss per Link (10^{-3}) ($AELL_l$) |
|-------------------------------|--|---|---------|---------|---------|---------|-----|--------|-----|---------|---|
| | | 1 | 2 | 3 | 4 | 5 | ... | 3,560 | ... | 12,000 | |
| 1 | 0.1519572 | 0 | 0 | 0 | 0 | 0 | ... | 0 | ... | 0 | 0.1515971 |
| 2 | 0.1519572 | 0 | 0 | 0 | 0 | 0 | ... | 0 | ... | 0 | 0.1635546 |
| 3 | 0.1519572 | 0 | 0 | 0 | 0 | 0 | ... | 0 | ... | 0 | 0.1531330 |
| 4 | 0.1519572 | 0 | 0 | 0 | 0 | 0 | ... | 0 | ... | 0 | 0.1894979 |
| 5 | 0.1519572 | 0 | 0 | 0 | 0 | 0 | ... | 0 | ... | 0 | 0.2126607 |
| ... | ... | ... | ... | ... | ... | ... | ... | ... | ... | ... | ... |
| 18,124 | 17.858600 | 0 | 0 | 0 | 0 | 0 | ... | 0 | ... | 1 | 0.1895587 |
| 18,125 | 17.858600 | 1 | 1 | 1 | 0 | 0 | ... | 0 | ... | 0 | 0.1737289 |
| Network Efficiency Loss (NEL) | | 0.01684 | 0.02624 | 0.04770 | 0.03999 | 0.02553 | ... | 0.1182 | ... | 0.01683 | |
| NEL in % | | 2.441 | 3.804 | 6.913 | 5.795 | 3.699 | ... | 17.133 | ... | 2.439 | |
| No. of Disruptions | | 121 | 109 | 142 | 136 | 126 | ... | 137 | ... | 128 | |

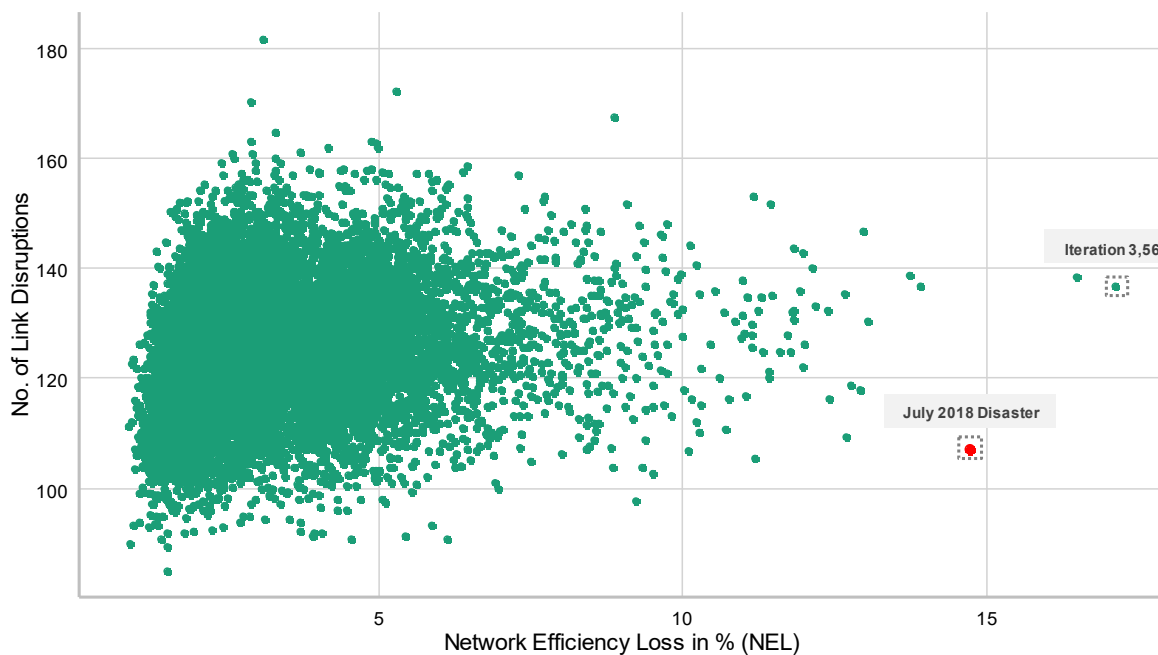


Fig.4 Comparison between number of disrupted links and network efficiency loss

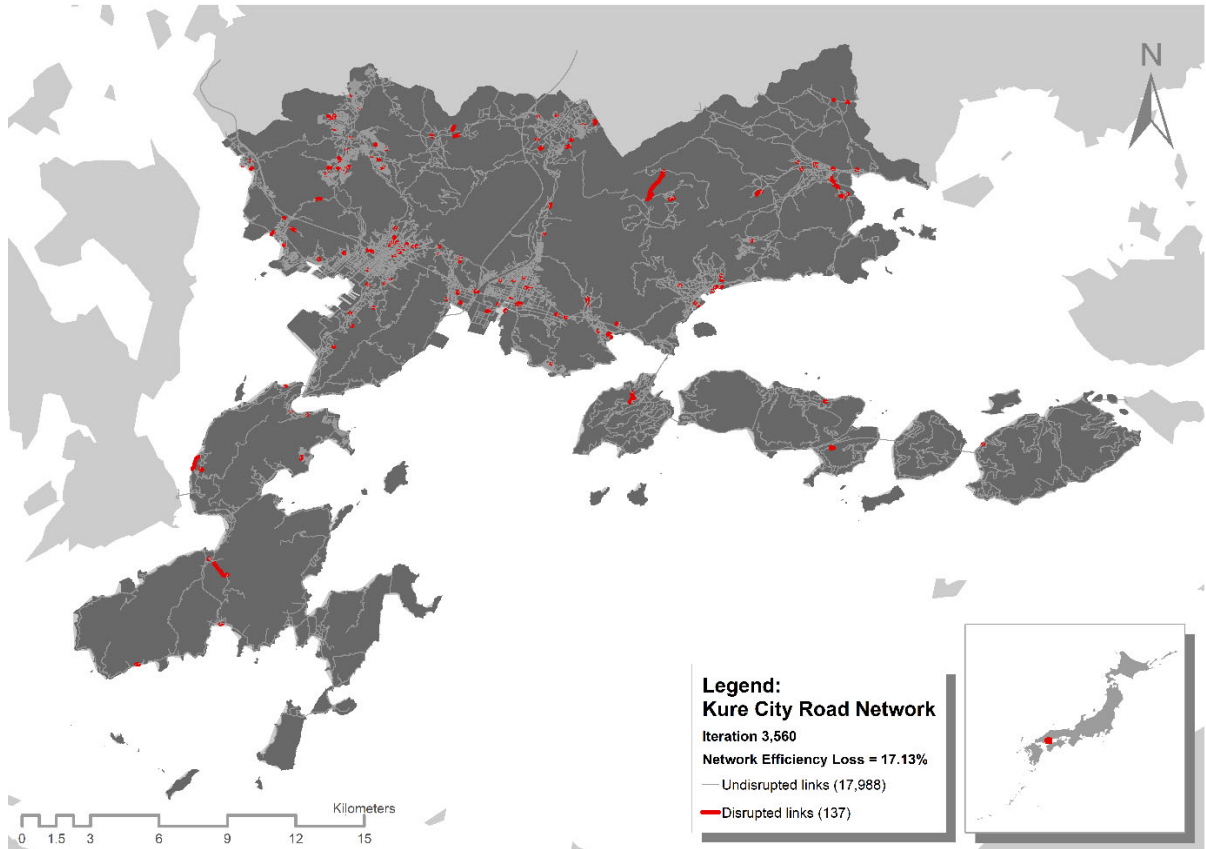


Fig.18 Highest impact scenario map (Iteration 3,560) in Kure City

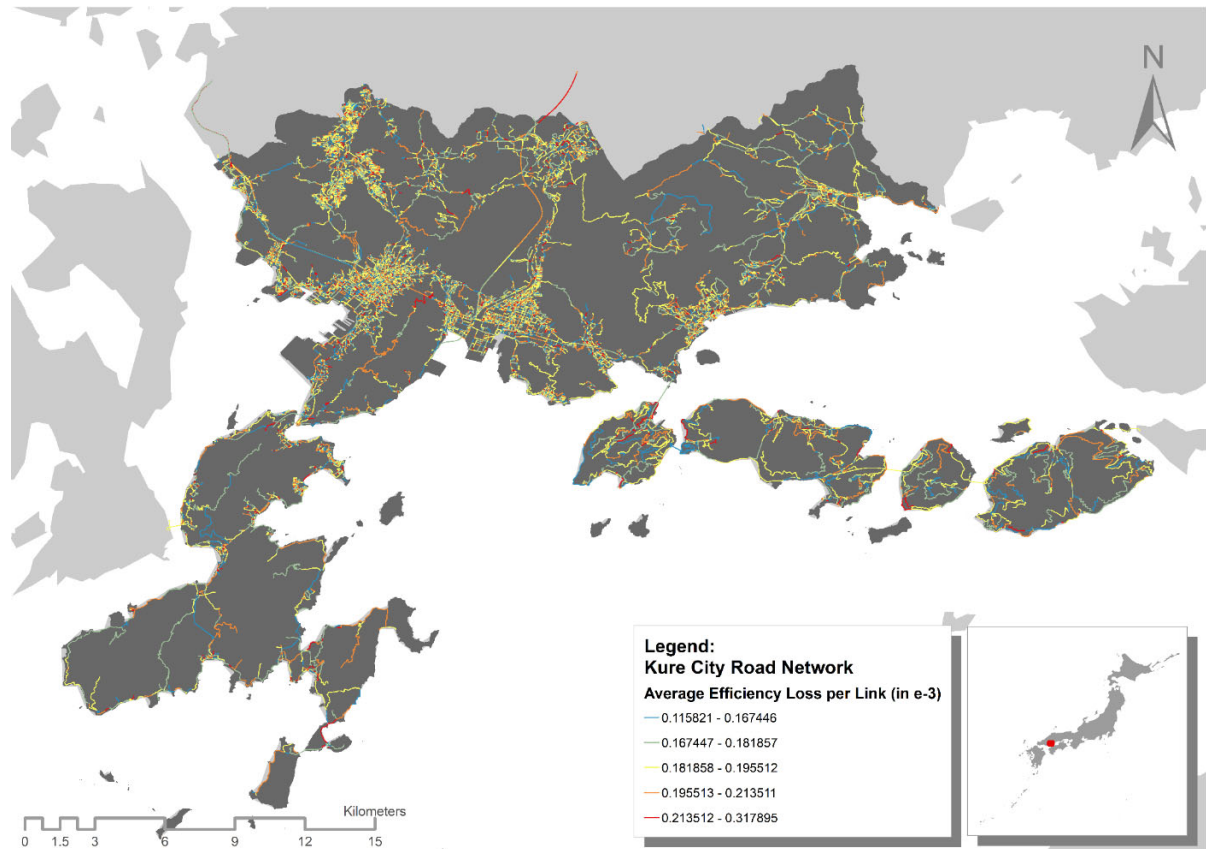


Fig.19 Impact map of Kure City

Meanwhile, the criticality of a road link depends on the disruption probability and impact, wherein if the probability of failure for a link is high, then the link maybe considered weak. If the impact of the link disruption is high, then the link is important. And if the link is both weak and important, then it is considered critical^{4,6)}. In this case, critical links may also be regarded as the high-risk links.

In Fig.23, inter-city road links in Kure City, specifically Route 31 (Hiroshima-Kure Road) and Route 375 (Higashihiroshima-Kure Expressway) are identified high-risk links. The importance of this finding suggests that the local government must provide further attention to this important links particularly because these are crucial in maintaining connectivity to adjacent cities. Furthermore, critical links in Kure City network may be prioritized in infrastructure investment allotment in order to ensure that communities within the city, or even the city itself, would not be isolated in the worst-case disaster scenario similar

to the July 2018 disaster.

However, the dynamics and combination of several links may also affect the observed impact as shown in the previous section, and thereby affect the calculated risk. It should also be noted that the risks computed for each link only reflects the risk from the topological vulnerability (network structure) and the sediment hazard exposure. In order to fully reflect the risk, it is recommended that the system-based vulnerability, which takes into consideration the travel demand, travel time and travel cost, may be studied as well.

Moreover, the generated risk maps are not intended to be an absolute guide for decision making which is bounded only between high-risk and low-risk links. The probability map and impact maps (see figures 15 and 19) may also be supplemental aid for policy makers in prioritization and tradeoff balance between high probability-low impact links, and low probability-high impact road segments.

Table 6 Risk calculation results

| Link | Occurrence Probability in % (OP_l) | Efficiency Loss per Link (ELL_l) (10^{-3}) | | | Risk ($OP_l \times ELL_l$) (10^{-6}) | | |
|--------|--|--|-----------|-----------|--|----------|----------|
| | | Min | Max | Ave | Min | Max | Ave |
| 1 | 0.1519572 | 0.08824554 | 0.2674726 | 0.1515971 | 0.013410 | 0.040644 | 0.023036 |
| 2 | 0.1519572 | 0.09262141 | 0.2622625 | 0.1635546 | 0.014074 | 0.039853 | 0.024853 |
| 3 | 0.1519572 | 0.06778412 | 0.4020616 | 0.1531330 | 0.010300 | 0.061096 | 0.023270 |
| 4 | 0.1519572 | 0.09641486 | 0.2562966 | 0.1894979 | 0.014651 | 0.038946 | 0.028796 |
| 5 | 0.1519572 | 0.1114081 | 0.2961352 | 0.2126607 | 0.016929 | 0.045000 | 0.032315 |
| ... | ... | ... | ... | ... | ... | ... | ... |
| 18,124 | 17.858600 | 0.07369177 | 0.4404158 | 0.1895587 | 1.316032 | 7.865210 | 3.385253 |
| 18,125 | 17.858600 | 0.07537948 | 0.4717958 | 0.1737289 | 1.346172 | 8.425612 | 3.102555 |

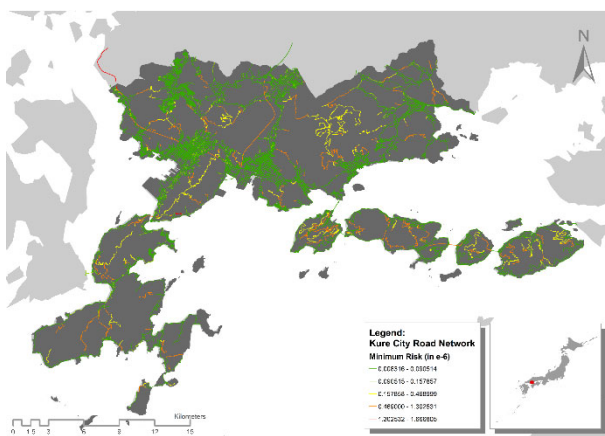


Fig.5 Minimum risk map of Kure City

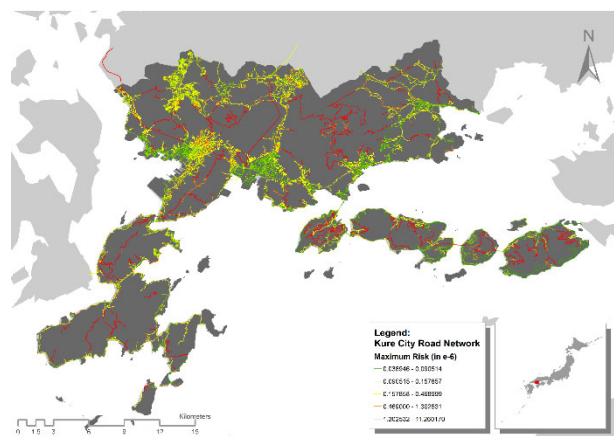


Fig.21 Maximum risk map of Kure City

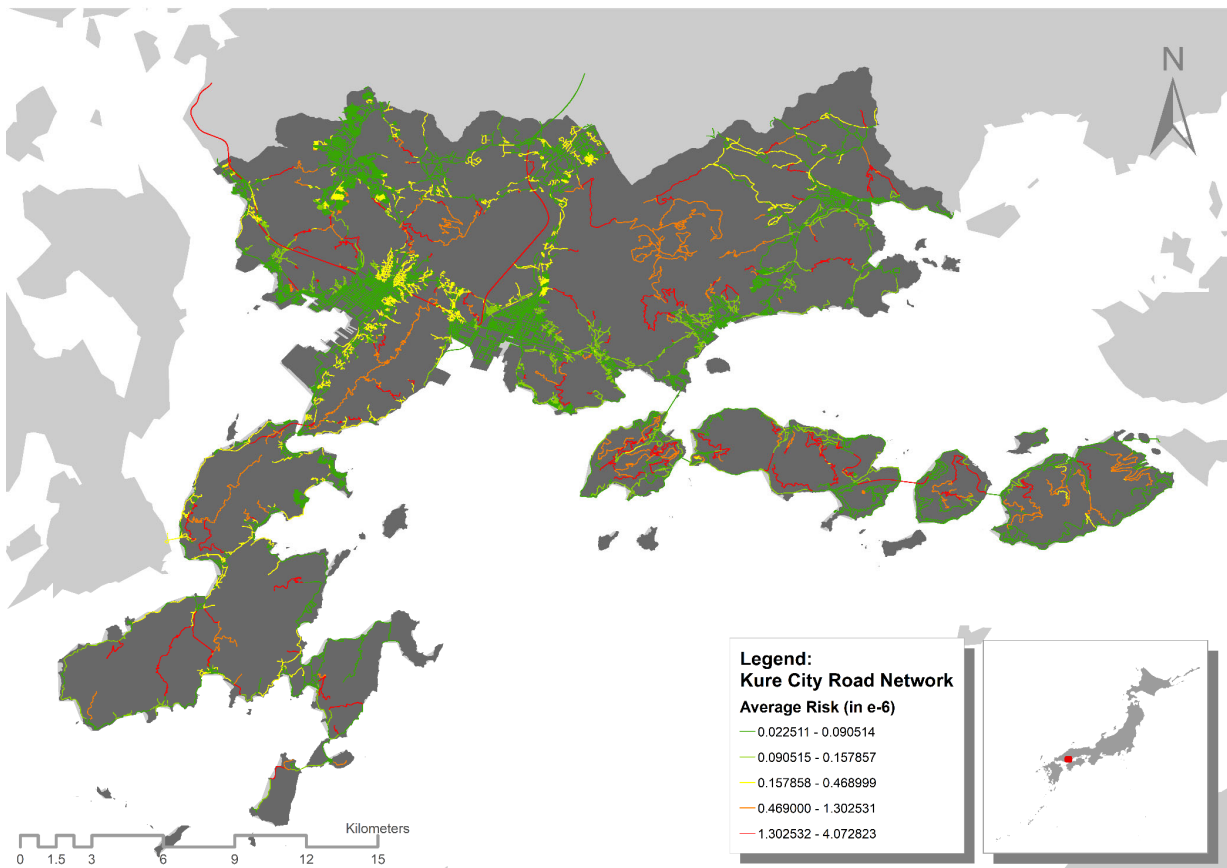


Fig.22 Average risk map of Kure City

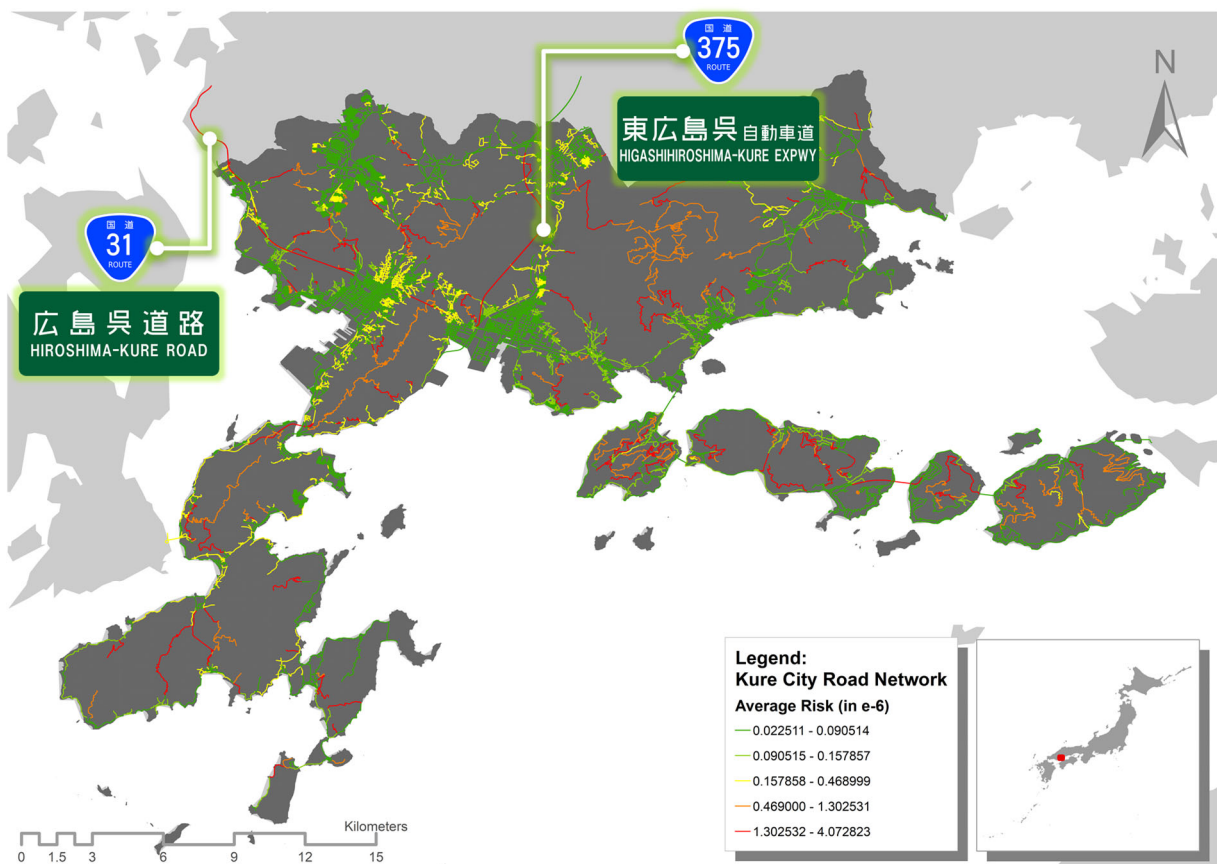


Fig.23 High risk inter-city road links in Kure City

5. CONCLUSION

In this research, the risk of sediment hazard was evaluated using a proposed risk assessment framework incorporating concepts from the fields of (1) transport vulnerability studies; (2) disaster risk assessment; and (3) spatial risk analysis. The proposed risk framework included the processes of topological network vulnerability analysis, hazard exposure spatial analysis, occurrence probability estimation through binary logit regression, and impact calculation using Monte Carlo simulation with 12,000 iterations. Subsequently, the framework was applied to an identified vulnerable road network in Kure City, Japan. Comparisons were made between the simulated link combination disruption scenarios and the July 2018 heavy rainfall disaster in Hiroshima prefecture. Simultaneously, different maps, including the occurrence probability map, impact map and risk maps, were generated to help identify high probable to hazard and high impact (i.e. high risk) road links in the road network.

The results of this study enable the (1) continuation of risk assessment development for road network; (2) emphasis on topological vulnerability analysis; (3) simplified disaster occurrence probability estimation, and (4) complete road network analysis for a whole medium-sized city. Similarly, the proposed framework can be improved and modified to accommodate other types of natural hazards, and further applied to other city road networks in the world. However, in each specific type of natural hazard, the exposure mapping and probability estimation would be entirely different. For the framework to be utilized, the exposure and probability analysis would need to be modified accordingly specific to the type of hazard being investigated by consulting specialized studies in that field.

Meanwhile, the proposed framework is not only limited for cities within Japan. While it is recognized that the availability and extent of data might not be as comparable as for developing countries, this study may provide the baseline data required in order to conduct an extensive analysis for a vulnerable road network. First and foremost, a complete road network GIS data, including street alleys to highways, is a basic prerequisite for topological vulnerability analysis. Second, an extensive database of past disaster event is needed to forecast future possible disaster scenarios. Lastly, these information can be further extended by gathering travel demand, travel time and travel cost data along all road links in the network. Possible policy implications of this study are further discussed in the next passage.

(1) Policy Implications

The policy implications of this research are three-fold. First, it can help in the disaster mitigation and recovery process. The output maps of the proposed framework could help in determining and prioritizing roads to be strengthened and recovered first during disaster. Maintaining connectivity in the road network during disaster is crucial for disaster response, including evacuation, rescue, and relief distribution, and restoration of other important infrastructure systems such as telecommunication, power, and water supply.

Second, the maps could complement existing systems used in road infrastructure investment. The identification of highly probable to hazard, high-impact and critical road segments could aid decision makers to properly allocate limited financial resources. This may also help in road transport decisions related to the expansion of the road network. Most infrastructure investment also relies on the results of cost-benefit analysis and the risk map may help shift or complement that perspective with risk-benefit analysis.

Finally, it could help in road transport management and road transport's internal and external connectivity improvement. Through the measurement of the topological characteristic, efficiency and vulnerability of a city's road network with its existing network structure condition, the local government may be provided with an insight on how their city fair in comparison to other city road networks and if further improvements may be needed to increase the connectivity within the road network. Moreover, through identification of high-impact road segments in the network, the local government may also determine the roads that provides the highest connectivity and would provide the greatest disfunctionality in the network if severed.

Nevertheless, these policy implications are not separate and are more often related to each other. Identifying critical links in the road network are important in order to maintain connectivity during disaster to ensure that communities would not be isolated. Meanwhile, high risk inter-city links should be strengthened further to guarantee that the city would readily receive disaster aid from nearby areas. Moreover, high-risk links (critical links), whether it is a local city road or inter-city link, might be further reinforced through allotting sufficient investment through widening or constructing redundant roads. In the case of Kure City, Route 31 (Hiroshima-Kure Road) and Route 375 (Higashihiroshima-Kure Expressway) are identified critical inter-city links that are crucial to maintaining connectivity to adjacent cities. Thus, the local government must strategize and align plans to strengthen these roads because of the risks from the topological vulnerability and hazard

exposure of Kure City. Nevertheless, looking only into the supply side (topology) of the road network might not be enough to quantify the over-all risk. Thus, several limitations of this study and recommendations for future studies are discussed in the next section.

(2) Limitations and Recommendations

While the aim of this study was to quantify the risks in a road network, the first limitation is that it only measured risk from the existing topological condition and potential hazard exposure of the road network. This study may be extended further to consider the actual transport demand by measuring vulnerability from the system-based approach with the extent and accuracy of big data analysis. Furthermore, this study only defined risk from the transportation perspective through the network efficiency loss indicator. Future studies may consider investigating potential risk of natural hazards to human life, social, and economic elements by including indicators like population, urban development and infrastructure facilities.

The proposed measurement of occurrence probability of sediment hazard may also have limitations compared to the prediction of those who specialize in geology engineering, geotechnical engineering and other fields that study sediment disaster. Until now, the measurement of hazard probability is still the subject of numerous studies outside the transportation field due to its complexity and uncertainty. Nevertheless, the estimation and calculation made in this study using numerous simulations provided meaningful insight for a whole city road network despite the data and resource limitations. In doing so, spatial correlation among the variables used to estimate the occurrence probability of sediment hazard should also be checked in future studies.

Furthermore, this study also tried to bridge the gap that exists between different fields that similarly assess risk, and which are theoretically interconnected. However, this study has only focused on one type of hazard. As discussed previously, a sediment disaster's occurrence relies on triggering factors that include other natural hazards like earthquake and heavy rainfall. It would be beneficial to examine multi-hazard combinations as this would pose a greater risk and impact not only for the road network but for the whole city as well.

REFERENCES

- 1) K. Berdica, "An introduction to road vulnerability: what has been done, is done and should be done," *Transport Policy* 10(2), pp. 117-127, 2003.
- 2) L.-G. Mattsson and E. Jenelius, "Vulnerability and resilience of transport systems – A discussion of recent research," *Transportation Research Part A* 81, pp. 16-34, 2015.
- 3) E. Dalziell and A. Nicholson, "Risk and Impact of Natural Hazards on a Road Network," *Journal of Transportation Engineering*, pp. 127(2): 159-166, 2001.
- 4) M. Taylor, *Vulnerability analysis for transportation Networks*, Cambridge: Elsevier Inc., 2017.
- 5) M. Anop, "Using Graph Model to Analyze the Topological Vulnerability of Transport Infrastructure," *DOOR*, 2016.
- 6) E. Jenelius, T. Petersen and L.-G. Mattsson, "Importance and exposure in road network vulnerability analysis," *Transportation Research Part A* 40, pp. 537-560, 2006.
- 7) J.-M. Tacnet, E. Mermet and S. Manceerat, "Analysis of importance of road networks exposed to natural hazards," in *AGILE'2012 International Conference on Geographic Information Science*, Avignon, 2012.
- 8) B. Michal, J. Sedonik, K. Jan, V. Rostislav, B. Martina and A. Richard, "Road Network Segments at Risk – Vulnerability Analysis and Natural Hazards Assessment," *The Science for Population and Protection*, vol. 2, 2014.
- 9) B. Postance, J. Hillier, T. Dijkstra and N. Dixon, "Extending natural hazard impacts: an assessment of landslide disruptions on a national road transportation network," *Environmental Research Letters*, p. 12 014010, 2017.
- 10) J. R. Santos, N. D. Safitri, M. Safira, V. Varghese and M. Chikaraishi, "Road Network Vulnerability and City-level Characteristics: A Nationwide Comparative Analysis of Japanese Cities," *Submitted to Environment and Planning B: Urban Analytics and City Science*, Vols. EPB-2020-0072, no. Manuscript submitted for publication, 2020 March 03.
- 11) T. A. Shimbun, "Kure residents cut off from outside world due to flooding," 10 July 2018. [Online]. Available: <http://www.asahi.com/ajw/articles/AJ201807100034.html>.
- 12) V. Latora and M. Marchiori, "Efficient Behavior of Small-World Networks," *Physical Review Letters*, vol. 87, no. 19, pp. 198701-1-4, 2001.
- 13) S. Porta, P. Crucitti and V. Latora, "The network analysis of urban streets: A dual approach," *Physica A*, vol. 369, p. 853–866, 2006.
- 14) X. Zhu, W. Song and L. Gao, "Topological Characteristics and Vulnerability Analysis of Rural Traffic Network," *Journal of Sensors*, p. Article ID 6530469, 2019.
- 15) Y. Duan and F. Lu, "Robustness of city road networks at different granularities," *Physica A* 411, pp. 21-34, 2014.
- 16) D. M. Scott, D. C. Novak, L. Aultman-Hall and F. Guo, "Network Robustness Index: A new method for identifying critical links and evaluating the performance of transportation networks," *Journal of Transport Geography*, pp. 215-227, 2005.
- 17) J. L. Sullivan, D. M. Scott and D. Novak, "Identifying critical road segments and measuring system-wide robustness in transportation networks with isolating links: A link-based capacity-reduction approach," *Transportation Research Part A* 44, p. 323–336, 2010.
- 18) A. Ganin, M. Kitsak, D. Marchese, J. Keisler, T. Seager and I. Linkov, "Resilience and efficiency in transportation networks," *Sciences Advances*, p. 3 : e1701079, 2017.
- 19) N. Haghghi, S. K. Fayyaz, X. C. Liu, T. H. Grubestic and R. Wei, "A Multi-Scenario Probabilistic Simulation Approach for Critical Transportation Network Risk Assessment," *Network Spat Econ*, pp. 18: 181-203, 2018.

- 20) E. Jenelius and L.-G. Mattsson, "Road network vulnerability analysis of area-covering disruptions: A grid-based approach with case study," *Transportation Research Part A*, vol. 46, pp. 746-760, 2012.
- 21) S. Lee and Y. Yoon, "Risk mapping of landslide hazard on road network," *Asian Journal of Research*, vol. 6, no. 6, pp. 74-115, 2017.
- 22) F. C. Dai, C. F. Lee and Y. Y. Ngai, "Landslide risk assessment and management: an overview," *Engineering Geology* 64, pp. 65-87, 2002.
- 23) J. Husdal, "Reliability and vulnerability versus costs and benefits," in *2nd International Symposium on Transport Network Reliability*, Christchurch & Queenstown, NZ, 2004.
- 24) United Nations International Strategy for Disaster Reduction (UNISDR), *2009 UNISDR Terminology on Disaster Risk Reduction*, Geneva, Switzerland: United Nations, 2009.
- 25) Intergovernmental Panel on Climate Change (IPCC), "Climate Change 2014: Impacts, Adaptation, and Vulnerability. Part A: Global and Sectoral Aspects. Contribution of Working Group II to the Fifth Assessment Report of the Intergovernmental Panel on Climate Change," Cambridge University Press, Cambridge, UK, 2014.
- 26) V. Ferretti and G. Montibeller, "An Integrated Framework for Environmental Multi-Impact Spatial Risk Analysis," *Risk Analysis*, pp. 39(1): 257-273, 2019.
- 27) "Earth and Sediment Disaster Caution Area," Hiroshima Prefectural Government, [Online]. Available: <https://www.sabo.pref.hiroshima.lg.jp>. [Accessed 21 May 2020].
- 28) "Information on July 2018 Disaster," Geospatial Information Authority of Japan, [Online]. Available: <https://www.gsi.go.jp/BOUSAI/H30.taihuu7gou.html#5>.
- 29) R. Kobashi, M. Kita, T. Uchida and Y. Kawahara, "Study on an evaluation method of initiation probability of debris flows during heavy rainfall," *Journal of Japan Society of Civil Engineers*, vol. 75, no. 1, pp. 191-199, 2019.
- 30) S. Derrible and C. Kennedy, "Characterizing metro networks: State, form and structure," *Transportation*, vol. 37, pp. 275-297, 2010.
- 31) S. Nakai, Y. Sasaki, M. Kaibori and T. Moriwaki, "Rainfall index for warning and evacuation against sediment-related disaster: Reexamination of rainfall index Rf, and proposal of R'," *Soils and Foundations*, vol. 46, no. 4, pp. 465-475, 2006.